Seismic tomography and mixing in the deep earth

W. R. Peltier, G. Pari, A. M. Dziewonski

Nonlinear Processes in Geophysics (1995) 2: 194 - 205

Nonlinear Processes in Geophysics

Seismic tomography and mixing in the deep earth

W. R. Peltier[1], G. Pari[1] and A. M. Dziewonski[2]

[1] Department of Physics, University of Toronto, Toronto, Ontario M5S 1A7, Canada
[2] Department of Earth and Planetary Sciences, Harvard University, Cambridge, MA 02138, USA

Received 26 June 1994 - Accepted 24 March 1994 - Communicated by L. Knopoff

Abstract.

Recently constructed tomographic models of the lateral heterogeneity of elastic properties in the Earth's mantle are contrasted in terms of their implications concerning the extent to which the endothermic phase transformation at 660 km depth is influencing the radial style of mixing. Previously published whole mantle and split mantle tomographic reconstructions, SH8/WM13 and SH8/U4L8 respectively, fit the seismic observations equally well but disagree on the extent to which radial mixing may be impeded across this depth horizon. We show that inferences from seismic tomographic images based on the application of diagnostic functions (global and regional variance spectra and the radial correlation function) lead to the conclusion that the mantle circulation is whole mantle in style if model SH8/WM13 is employed. The split mantle tomographic inversion SH8/U4L8 leads to the contradictory conclusion that the mantle circulation is significantly impeded across the 660 km depth horizon. This latter interpretation is reinforced when we employ the new higher resolution split mantle model SH12/U7L5 in our calculations. We demonstrate that the depth-dependent radial heat flow delivered by both of the split models implies the existence of a thermal boundary layer at 660 km depth, and therefore significant layering, whereas that delivered by the whole mantle model does not. By insisting that the depth-dependent viscosity profile of the mantle be compatible with the thermal structure if the flow were layered, we argue that the split mantle tomographic inversions lead to a self-consistent description of geodynamic constraints (geoid and postglacial rebound data).

1 Introduction

The issue of the radial structure of the thermal convective circulation that fills the earth's mantle and that is responsible for driving the relative motion of the surface plates is as yet unresolved (Peltier et al., 1989; Olson et al., 1990). The key question concerns the impact on radial mass transport of the endothermic phase transformation of γ-spinel to a mixture of perovskite and magnesiowüstite that occurs near the depth of 660 km. Recent analyses of the magnitude of this effect based upon large scale numerical simulations have demonstrated that when the Clapeyron slope of this transformation is fixed to the experimentally observed value of -4 ± 2 MPa/°K (Ito et al., 1990), the influence of the phase transition is profound (Machetel and Weber, 1991; Peltier and Solheim, 1992; Solheim and Peltier, 1993; Zhao et al., 1992; Tackley et al., 1993; Solheim and Peltier, 1994a, 1994b).

In axisymmetric spherical geometry the effect of this phase transition is to cause the flow regime to become strongly time dependent (Machetel and Weber, 1991; Peltier and Solheim, 1992; Solheim and Peltier, 1993, 1994a, 1994b). The extensive intervals of layered convection that result are episodically disrupted by the occurrence of intense "avalanches" of cold material that descend from the base of the transition zone into the lower mantle (Machetel and Weber, 1991; Peltier and Solheim, 1992; Solheim and Peltier, 1993, 1994a). This temporal episodicity is controlled by the creation and destruction of an instability of the thermal boundary layer that develops across the endothermic horizon itself (Solheim and Peltier, 1994b). Since the quasi-period separating successive excursions from the layered state into the whole mantle state is near 600 Myr when the Rayleigh number is fixed to the earth-like value of 10^7, the avalanche process might be expected to play an important role in driving the so-called Wilson cycle of ocean basin opening and closing as well as controlling the episodes of orogeny that accompany this supercontinent cycle.

In three dimensional spherical geometry (Tackley et al., 1993), the quasi-periodicity of the avalanche events is significantly muted from that evident in the axisymmetric model, since at any one time a large number of

Correspondence to: W. R. Peltier

avalanches are occurring and these are not correlated with respect to the stage of their individual life cycles. Rather than being indicative of a serious flaw in the dynamical characteristics of the two dimensional model, however, this decorrelation could be a consequence of the fact that the chosen value of 2×10^6 for the Rayleigh number in the 3-dimensional simulations is considerably below the value of 10^7 which is characteristic of the modern earth (the propensity for layering was found to increase as a function of increasing Rayleigh number in the 2-dimensional axisymmetric simulations of Solheim and Peltier (1994a), an observation which was also made previously, at lower Rayleigh number and in 2-dimensional cartesian box geometry, by Christensen and Yuen (1985)). Perhaps more importantly, the influence of surface plates is more strongly controlling of the flow in three dimensions and this control works in such a way as to reduce the number of active downwellings in the system and thereby increase their individual importance. The latter influence is not included in any of the extant models.

Whether the endothermic phase transformation at 660 km depth might have a similarly controlling influence on the radial mixing process in the real Earth as that evidenced in the 2 and 3 dimensional numerical simulations cited above is the principal question we wish to address in this paper. The main global observational data that might reasonably be invoked to investigate this issue consists of seismic tomography models of the three dimensional elastic structure of the mantle. In attempting to employ such models for this purpose, however, we must first identify what feature or features might best be employed as diagnostic of the phase transition effect.

Probably the most highly diagnostic characteristic of this effect that has as yet been suggested consists of the depth-dependent variance of the lateral heterogeneity of seismic body wave velocity. This has been shown to develop a sharp peak centered on the endothermic horizon at times when the coincident thermal boundary layer is well developed and the flow is in a predominantly layered state (Peltier and Solheim, 1992). More recently, the depth-dependent autocorrelation function has also been proposed as an equally appropriate discriminant (Jordan et al., 1993). When applied to the three dimensional spherical simulation of Tackley et al. (1993), which is characterized by a strong phase transition effect, it was shown that the radial correlation function developed an evident minimum at the depth of the endothermic horizon. This feature was shown not to be present in the whole mantle tomographic reconstructions SH12/WM13 (Su et al., 1994) and SH10C (Masters et al., 1992), and it was therefore concluded by Jordan et al. (1993) that the phase transition effect must be much weaker in the real earth than it is in the model of Tackley et al. (1993). A further diagnostic measure of the strength of the phase transition effect that has been employed in all recent simulations of mantle mixing is the azimuthally integrated radial mass flux that was first introduced by Peltier and Solheim (1992) where it was shown to develop a pronounced local minimum at the depth of the endothermic horizon. This diagnostic has recently been applied directly to global tomographic models, constructed from the observed magnitude of the topography on the 660 km discontinuity (Shearer and Masters, 1992) and tomographic models SH8/WM13 (Woodward et al., 1993) and SH10C (Masters et al., 1992), by Morgan and Shearer (1993). They have concluded, on the basis of the absence of a local minimum in the radial mass flux, that the mantle circulation must be operating in an essentially whole mantle mode at present, implying either that the phase transition effect is much weaker in the real earth than in either the axisymmetric or the three dimensional convection models, or that the flow is presently in a transient state of whole mantle circulation.

Our analyses in what follows suggest that the arguments that have been presented to the effect that the phase transition effect must be weak in the real earth might not be well-founded. Since the tomographic models considered by both groups of authors (Jordan et al., 1993; Morgan and Shearer, 1993) impose a smooth variation of the heterogeneity field across the 660 km discontinuity, there is clearly an explicit bias in these analyses towards the "whole mantle conclusion". Our analyses in the present paper have been designed to look critically at these previous discussions and are based in part upon the explicit demonstration of the non-uniqueness inherent to the tomographic inversions. We will show that the split mantle tomographic model SH8/U4L8 (Dziewonski and Woodward, 1992) as well as a new high resolution split mantle model SH12/U7L5 imply the occurrence of significant layering across the endothermic horizon. These analyses will begin with consideration of the total and spatially disaggregated depth-dependent variance associated with the lateral heterogeneity field. We will also find that significant layering is implied by a reconsideration of the analysis of Jordan et al. (1993) when it is applied to a split model. The layered convection scenario suggested by these results implies the existence of a thermal boundary layer at 660 km depth. We propose that a particularly useful diagnostic that may be employed in the search for this boundary layer is the depth-dependent profile of the radially advected heat (Pari and Peltier, 1993, 1995). When the split mantle tomographic models are used in our calculation of the advected heat flow, a sharp drop is revealed at 660 km depth, as would be expected in a region where heat is primarily transported by conduction rather than by convection.

In summarizing the results of these analyses in Section 4 of this paper, we will therefore conclude that the scenario in which the convective circulation is significantly layered by the action of the endothermic phase transition is not ruled out by the data but neither can

the data that we analyse be construed to require that the flow be of this form.

2 On the diagnosis of layered convection is seismic tomographic images

2.1 Split mantle tomography vs whole mantle tomography

On the basis of recent seismic tomographic reconstructions of three dimensional mantle elastic structure, it is quite clear that there exists a non-negligible dependence of the models recovered as solutions to the inverse problem upon the functional parameterization employed to represent this structure. A striking example of this has been provided by Dziewonski and collaborators in their models SH8/WM13 and SH8/U4L8 (Woodward et al., 1993; Dziewonski and Woodward, 1992). Although both models are formulated in terms of spherical harmonic expansions to degree and order 8, the depth dependence of the former is represented on a single basis of Chebyshev polynomials to degree 13 whereas for the latter, it is represented by distinct Chebyshev expansions to degrees 4 and 8 respectively above and below 660 km depth. Clearly the split mantle parameterization will allow for the development of maximal structure in the retrieved model at 660 km depth whereas the whole mantle representation will mitigate against the occurrence of such anomalous structure.

There is therefore a clear issue as to which parameterization we should select on a-priori grounds as being best suited to the recovery of any phase transition related structure that may exist in the real earth. One might argue either that the smooth model SH8/WM13 is most appropriate since if structure should appear in spite of the smoothing inherent to the parameterization then it is definitely present; or equally, and on the contrary, that the split parameterization is most appropriate because it gives the latitude for the development of phase transition related structure that may otherwise be filtered due to the low spatial resolution at which the tomographic inversions must be performed. It is important to realize that both the whole mantle and split tomographic models fit the seismic constraints equally well (Woodward et al., 1993; Dziewonski and Woodward, 1992), and on these grounds alone, there is no logical basis on which the split model should be ignored in favour of that delivered by a whole mantle parameterization.

2.2 Global and regional variance spectra

In order to show that this issue is not inconsequential, we first compare in Figure 1 the depth-dependent power spectra of models SH8/WM13 and SH8/U4L8. The depth-dependent power spectrum p_Ω is defined by the

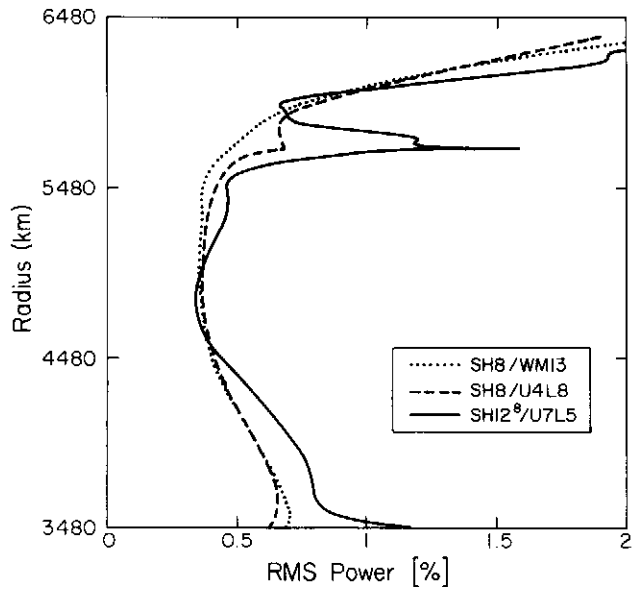

Fig. 1. The depth-dependent globally averaged root mean square power spectrum (text equation 1) for tomographic models SH8/WM13 (dotted line), SH8/U4L8 (dashed line) and SH12^8/U7L5 (solid line).

familiar expression

$$p_\Omega(r)^2 = \int\int_\Omega \left|\frac{\delta V_s}{V_s}\right|^2 d\Omega = \sum_{lm} \left|\left(\frac{\delta V_s}{V_s}(r)\right)_{lm}\right|^2, \quad (1)$$

in which the integral of the square of the lateral heterogeneity field $\delta V_s/V_s$ is carried out over the surface of the sphere Ω. The last equality in Eq. 1 is obtained by expressing

$$\frac{\delta V_s}{V_s}(r,\theta,\phi) = \sum_{lm} \left(\frac{\delta V_s}{V_s}(r)\right)_{lm} Y_{lm}(\theta,\phi) \quad (2)$$

and employing the orthogonality relation for the spherical harmonic basis functions $Y_{lm}(\theta,\phi)$. We find that for tomographic model SH8/WM13, this diagnostic function is a smooth function of depth that shows no evidence of the sharply focused peak in variance at 660 km that the convection models suggest should exist if the endothermic phase transformation is playing an important role (Peltier and Solheim, 1992). On the other hand the spectrum for model SH8/U4L8 does reveal, if in a somewhat muted form, anomalous structure centered on this horizon. Is this peak to be considered simply an artifact of the split parameterization? We address this issue in Figure 2 where we show a more detailed analysis of a result recently obtained by Woodward et al. (1994) concerning the regional variation of the depth-dependent power spectrum in the smooth model SH8/WM13.

This depth-dependent power spectrum is calculated by laterally averaging the square of the heterogeneity

field $\delta V_s/V_s$ over spherical caps $C^{\theta_0}_{\Theta,\Phi}$ of angular radius θ_0 centered at latitude-longitude coordinates (Θ, Φ) and subtended by cones with apex located at the center of mass of the earth. In contradistinction with the work of Woodward et al. (1994) which was based upon numerical integration of the power spectrum over the spherical caps $C^{\theta_0}_{\Theta,\Phi}$, we present an analytical derivation leading to a simple expression for the regional power spectrum in terms of Wigner 3-j symbols. The first step in the derivation consists in expressing the square of the power spectrum as an expansion in terms of spherical harmonics:

$$p(r,\theta,\phi)^2 = \left|\frac{\delta V_s}{V_s}(r,\theta,\phi)\right|^2 = \sum_{lm} \alpha_{lm}(r) Y_{lm}(\theta,\phi) \qquad (3)$$

in which

$$\alpha_{lm} = \sum_{l'm'l''m''} \left(\frac{\delta V_s}{V_s}\right)_{l'm'} \left(\frac{\delta V_s}{V_s}\right)^*_{l''m''} \times \int\int_\Omega Y_{l'm'} Y^*_{l''m''} Y^*_{lm}\, d\Omega\,. \qquad (4)$$

The integral over the triple product of spherical harmonics can be expressed in terms of Wigner 3-j symbols (Edmonds, 1974), leading to the following form for α_{lm}

$$\alpha_{lm} = \sum_{l'm'l''m''} \left(\frac{\delta V_s}{V_s}\right)_{l'm'} \left(\frac{\delta V_s}{V_s}\right)^*_{l''m''} \times (-1)^{m+m'} \left[\frac{(2l'+1)(2l''+1)(2l+1)}{4\pi}\right]^{1/2} \times \begin{pmatrix} l' & l'' & l \\ 0 & 0 & 0 \end{pmatrix} \begin{pmatrix} l' & l'' & l \\ m' & -m'' & -m \end{pmatrix}. \qquad (5)$$

By rotating the coordinate system so that the original z-axis now points along the direction of the symmetry axis of the cone, we can simplify the integral of a spherical harmonic function over the spherical cap. Since spherical harmonics form an irreducible representation of the group of rotations, there exists complex coefficients D^l_{mn} (the standard rotation matrices (Edmonds, 1974)) which link two representations of this group, namely:

$$Y_{lm}(\theta,\phi) = \sum_{n=-l}^{l} D^l_{mn}(\Theta,\Phi,\Psi) Y_{ln}(\theta',\phi')\,. \qquad (6)$$

The angles Θ, Φ, Ψ are Euler angles which perform the necessary coordinate transformation from the θ, ϕ frame to the θ', ϕ' frame defined by the symmetry axis of the cone. By employing the fact that rotations are unitary transformations, we arrive at the desired result:

$$\int\int_{C^{\theta_0}_{\Theta,\Phi}} Y_{lm}(\theta,\phi)\, d\Omega = 2\pi\, D^l_{m0}(\Theta,\Phi,\Psi=0) \times \int_0^{\theta_0} Y_{l0}(\theta') \sin\theta' d\theta', \qquad (7)$$

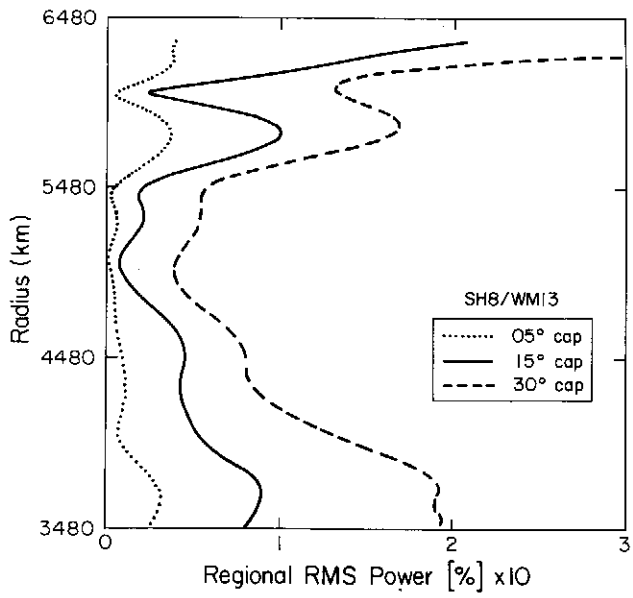

Fig. 2. The depth-dependent regional power spectrum (text equation 8) for tomographic model SH8/WM13. The dotted line corresponds to 5° caps, the solid line to 15° caps and the dashed line to 30° caps. All caps are centered at latitude 22° N and longitude 137° E, corresponding to an active zone of subduction (Tonga Trench).

which, when applied to the regional power spectrum case, yields

$$p_{C^{\theta_0}_{\Theta,\Phi}}(r)^2 = \int\int_{C^{\theta_0}_{\Theta,\Phi}} \left|\frac{\delta V_s}{V_s}\right|^2 d\Omega = \sum_{l,m} \left(\frac{16\pi^3}{2l+1}\right)^{1/2} \times (-1)^m \alpha_{lm}(r) Y_{lm}(\Theta,\Phi) \int_0^{\theta_0} Y_{l0}(\theta') \sin\theta' d\theta'. \qquad (8)$$

To write this last expression, we have employed the fact that the rotation matrix D^l_{m0} is, up to a phase factor and renormalisation constant, proportional to a spherical harmonic function (Edmonds, 1974).

Application of these analytical results clearly demonstrates that although the full spherical average of the depth-dependent power spectrum is smooth for model SH8/WM13 (as on Figure 1) there are nevertheless geographical regions, even in this smooth model, in which the expected phase transition effect is clearly evident. In Figure 2 the depth-dependent spectrum that is most meaningful, given the horizontal resolution of the tomographic model, is that for which the integral is performed over a spherical cap of angular radius 15°. The result shown in Figure 2 is centered on the Tonga Trench; we are currently preparing a detailed analysis of the geophysical inferences, and their significance, made by employing our regional disaggregation of the power spectrum. Since even the smooth model contains the phase transition effect as a local feature in some geographic locations, it does seem reasonable to enquire, as is effectively done by employing the split parameterization, as

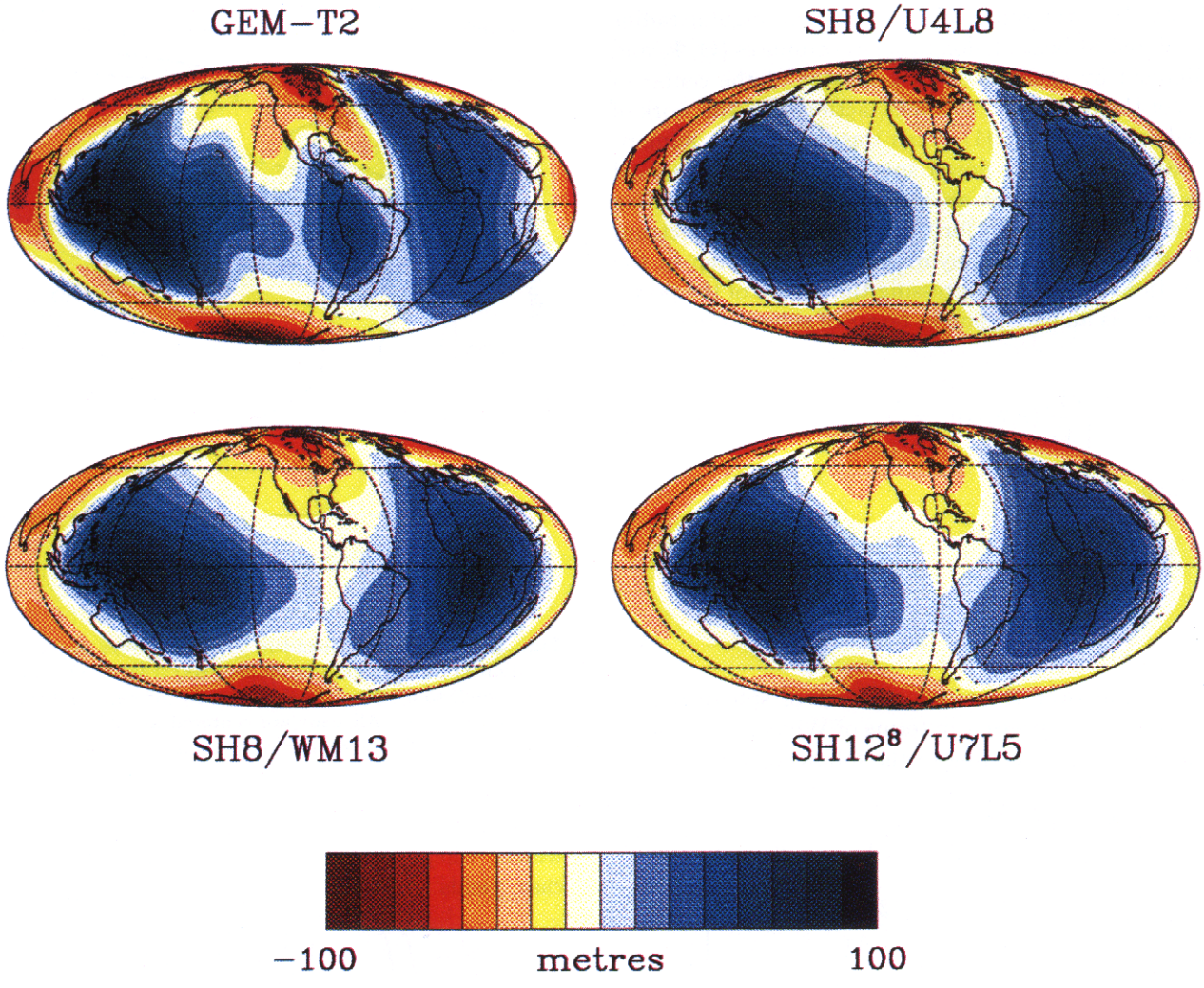

Fig. 3. Surface map reconstructions of the degree 2 to 8 observed nonhydrostatic GEM-T2 geoid and degree 2 to 8 geoids calculated using tomographic models SH8/WM13, SH8/U4L8 and SH12^8/U7L5. Note that for the theoretically predicted fields, the degree two and order zero component has been set equal to the observed value. This is justified by virtue of the results of simultaneous inversions of seismic and geodynamic data which demonstrate that the main cause of the degree 2 and order 0 mismatch that otherwise obtains is due to poor seismic coverage of the southern hemisphere (Forte et al., 1994). The variance reductions obtained before and after this adjustment are respectively 56 % and 80 % for SH8/WM13, 60 % and 81 % for SH8/U4L8, 56 % and 84 % for SH12^8/U7L5.

to how much more strongly developed this feature might become if it were allowed maximal freedom to do so.

In this spirit, we have elected to test the robustness of the result obtained with the split parameterization SH8/U4L8 by considering a new higher resolution split model SH12/U7L5. In this new model, the lateral heterogeneity is represented on a basis of spherical harmonics truncated at degree and order 12 whereas the radial structure is represented by Chebyshev expansions truncated at degree 7 in the upper mantle and degree 5 in the lower mantle. The seismic data set used in this new inversion has been enlarged by nearly a factor of three with respect to that previously described (Woodward et al., 1993; Dziewonski and Woodward, 1992). Even in comparison with the data set employed in the study of Su et al. (1994), this new model includes information from more recently installed stations and the waveform data that are inverted span a greater frequency range. A complete presentation of the details that enter in the construction of this seismological inversion will be given elsewhere by Dziewonski. For the purpose of this work, we point out that model SH12/U7L5 achieves significantly better variance reduction of the expanded data set than does either SH8/WM13 or SH8/U4L8.

In Figure 1, we show the power spectrum of the lateral heterogeneity which characterizes this preferred seismic model. The peak in spectral power that was only weakly developed in the lower resolution model SH8/U4L8 not only still exists but is strongly enhanced in this higher resolution model. In SH12/U7L5 the expected spectral

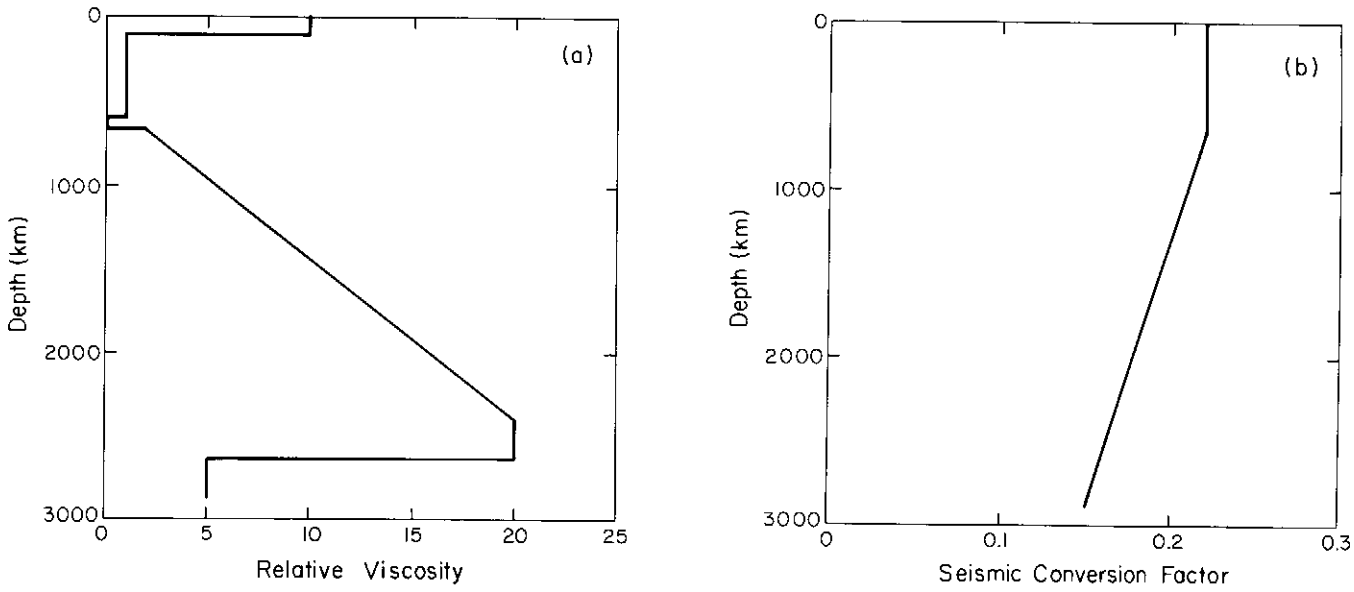

Fig. 4. Viscosity profile (Plate a) and s-wave seismic conversion factor (Plate b) used for all calculations presented in the text. The low-viscosity notch above the 660 km discontinuity has a thickness of 70 km and a viscosity $\nu = 0.02$ (the upper mantle viscosity, which is the reference value, is set equal to unity).

signature of the phase transition effect is as strongly developed as a-priori models of the mantle convection process have implied (Peltier and Solheim, 1992; Tackley et al., 1993). The (degree) disaggregated contour plots of the variance spectrum presented in Figure 5 (left column) tell a similar story. No excess in power at the depth of 660 km is revealed for model SH8/WM13 at any degree. Although at that depth model SH8/U4L8 shows a slight increase in variance at low degrees, it is in model SH12/U7L5 that this peak is fully developed. The significant low degree power present at this depth in this new model makes the associated transition zone heterogeneity stand out as one of the more prominent aspherical anomalies of the mantle, an observation reminiscent of the early results of Masters et al. (1982).

2.3 The nonhydrostatic geoid

That all of these tomographic models provide equally satisfactory reconciliations of the observed degree 2 to 8 non-hydrostatic geoid is demonstrated in Figure 3 on which we compare the predictions of this field obtained using the compressible flow theory of Forte and Peltier (1991) with the observed GEM-T2 geoid (Marsh et al., 1990). The harmonic coefficients of the geoid g_{lm} are computed according to the now-standard expression (Hager and Richards, 1989; Forte and Peltier, 1991)

$$g_{lm}(r) = \frac{3}{2l+1} \int_b^a G^l(r_e, r')\, \delta\rho_{lm}(r')\, dr', \qquad (9)$$

in which G^l denotes the (dimensionful) deflection due to a unit mass load located at mantle radius r' of the model's ocean surface. The integration is carried out from the core-mantle boundary $r = b$ to the outer solid surface of the Earth located at $r = a$ and r_e denotes the average radius of the Earth. The density heterogeneity $\delta\rho$ is assumed to be of thermal origin only and is obtained from the seismic shear-wave velocity anomalies $\delta V_s/V_s$ through the use of a depth-dependent parameter $\partial \ln \rho / \partial \ln V_s$ (see Eq. 12 below). Another depth-dependent parameter of the model which is employed in this comparison, the radial profile of mantle viscosity, is similar to that presented previously in Forte et al. (1993) whereas the seismic conversion factor $\partial \ln \rho / \partial \ln V_s$ is somewhat modified. Both of these characteristics of our model are shown in Figure 4 (Plates a and b respectively).

From Figure 3, we see that the most prominent features of the observed geoid, in particular the geoid highs centered over the West coast of Africa and to the North of Australia as well as the geoid lows over Hudson Bay and Antarctica, are obviously well represented by both the whole mantle and the split models (variance reductions are provided in the caption to Figure 3). We are therefore unable to discriminate between their quality on this basis. It is clearly of interest to enquire whether some further diagnostics might exist that would be as valuable as the depth-dependent power spectrum in this regard.

2.4 The Radial correlation function

One means that we might reasonably employ to further analyse the relative likelihood of the three models SH8/WM13, SH8/U4L8, and SH12/U7L5 is the radial correlation function first introduced in this context by

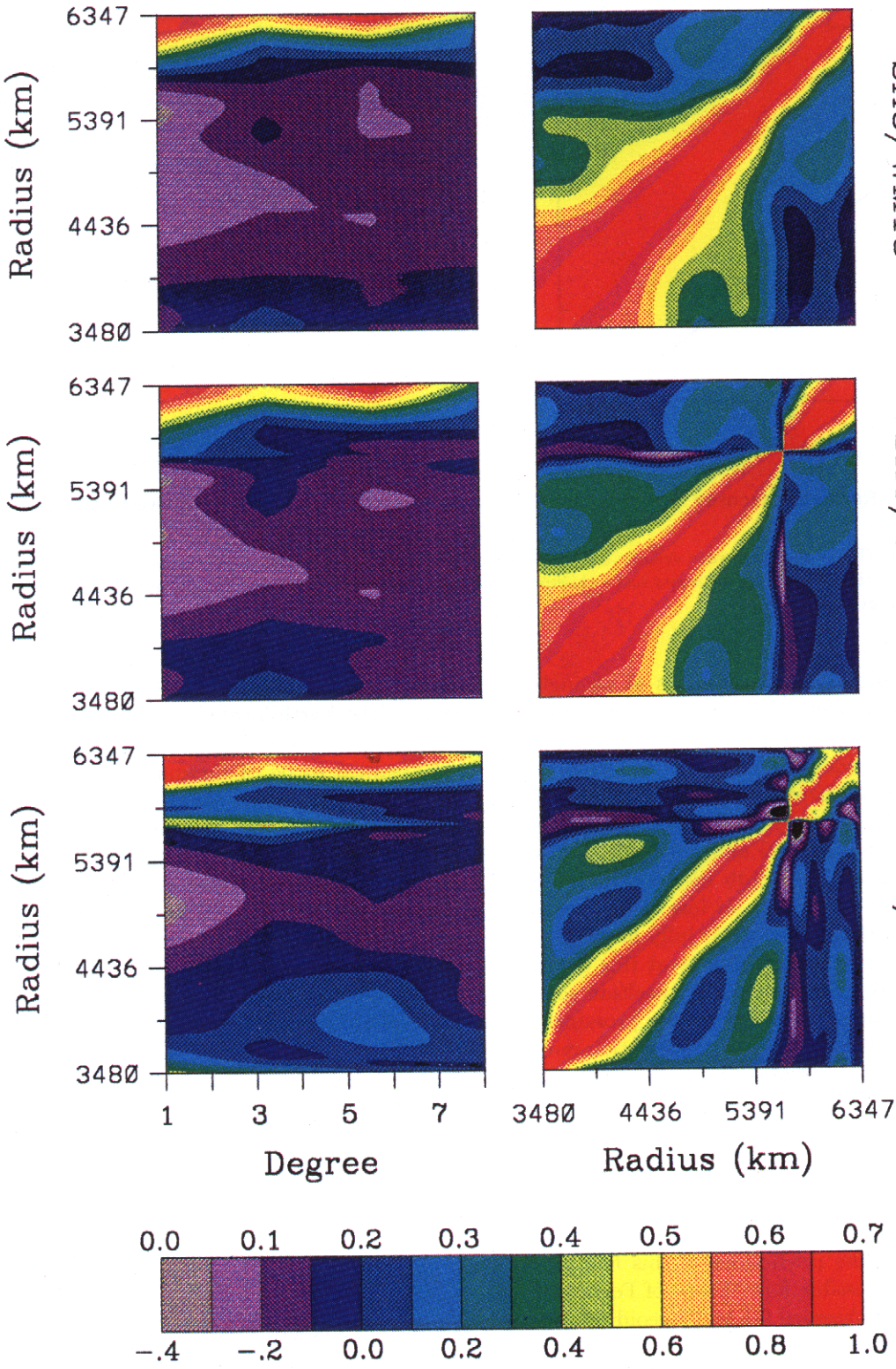

Fig. 5. Degree disaggregated root mean square amplitude of the heterogeneity field (left column) and the radial correlation (right column, text equation 10) for tomographic models SH8/WM13, SH8/U4L8 and SH12^8/U7L5. Both scales are dimensionless: the one above the color bar corresponds to r.m.s. percentage and is associated with the amplitude plots whereas the one below is associated with the correlation plots. Saturation of the negative scale is indicated in black.

Jordan et al. (1993). This diagnostic function, which is defined by

$$\Gamma(r,r') = \int\int_{\Omega} \left(\frac{\delta V_s}{V_s}\right)(r,\theta,\phi)\ \left(\frac{\delta V_s}{V_s}\right)^{*}(r',\theta,\phi)\ d\Omega \div [\ p_{\Omega}(r)\ p_{\Omega}(r')\ ], \quad (10)$$

in which $p_{\Omega}(r)$ is defined in Eq. 1, provides information concerning the relative phase of heterogeneity fluctuations located on different spherical horizons of radius r and r'. It is normalised so that perfectly correlated horizons yield a diagnostic value of 1. On Figure 5 (right column) we therefore show this diagnostic for the three tomographic models we are employing. The results for model SH8/WM13 are similar to those obtained previously by Jordan et al. (1993) using whole mantle tomographic models. They show that the correlation length near 660 km depth is similar to that of other mantle depths. On this basis, it was concluded, by comparison with the equivalent diagnostic computed from the density field in the three dimensional convection model of Tackley et al. (1993), that the influence of the phase transition on convective mixing in the real earth must be minimal. For the split model SH8/U4L8, however, this diagnostic function is now characterized by a sharp drop in correlation between radial horizons located above and below the 660 km discontinuity. This is just the feature that one would expect if the influence of the phase transition were strong (Jordan et al., 1993).

The decorrelation across 660 km depth is even more strikingly expressed in model $SH12^8$/U7L5 as is also shown in Figure 5 (by $SH12^8$ we represent a degree 8 truncation of the high resolution split reconstruction SH12/U7L5). On the basis of this comparison we must conclude that the inference of Jordan et al. (1993) to the effect that their analysis rules out the operation of a strong impediment to radial mixing due to the endothermic phase transformation at 660 km depth might not be well-founded.

3 Radial mass transport, radial heat flow and layered convection

3.1 The radial mass flux diagnostic

A further diagnostic tool that has been employed in an attempt to address the issue of layered vs. whole mantle convection on the basis of mantle tomography consists of the radial mass flux diagnostic (Peltier and Solheim, 1992). Morgan and Shearer (1993) have recently computed this diagnostic using an incompressible mantle flow model and the three-dimensional density heterogeneity field inferred from whole mantle tomographic models SH8/WM13 and SH10C modified to include density anomalies associated with the observed deflection of the 660 km boundary (Shearer and Masters, 1992). On this basis they conclude that there is no evidence for any inhibition of the radial mass flux at 660 km depth and therefore no evidence for the operation of the strong influence of the phase transformation.

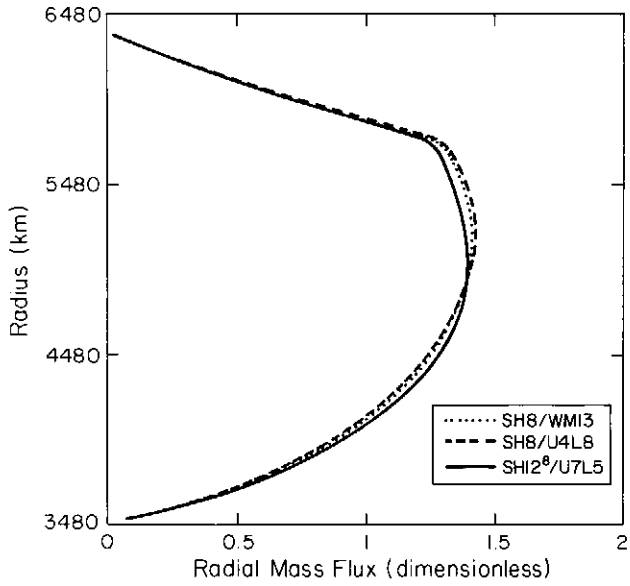

Fig. 6. The normalized radial mass flux diagnostic $\mathcal{M}(r)$ (text equation 14) as a function of mantle radius. The dotted line corresponds to SH8/WM13, the dashed line to SH8/U4L8 and the solid line to $SH12^8$/U7L5.

We have recomputed the radial mass flux diagnostic using the compressible flow theory of Forte and Peltier (1991) in conjunction with the viscosity and seismic conversion factor profiles of Figure 4. Here, our approach differs from that of Morgan and Shearer in that no modification to the global tomographic models was attempted in order to include possible effects of dynamic topography at 660 km. Including such effects on the basis of the Morgan and Shearer prescription is a perilous exercise. For example, double counting could be a problem since a significant fraction of the heterogeneity imagined to be associated with the phase deflection itself may already be present in the tomographic model. Also, an unphysical flow regime ensues: Morgan and Shearer (1993) point out that in some cases the calculated flow field is anticorrelated, over regions of significant geographical extent, with the 660 km dynamic topography map in contradiction to the physical situation which requires regions of hot upwelling (cold downwelling) material to be well-correlated with upwards (downwards) deflections of the 660 km boundary. This situation, which perhaps originates in inaccuracies present in the observed 660 km topography map or in the long-wavelength nature of the calculated flow which is necessarily organised on a whole-mantle scale, implies that in some cases the imagined 660 km heterogeneity actually helps drive the flow across 660 km rather

than impede it. Ultimately, the issue of properly including density heterogeneities associated with phase boundary deflections will have to await a global tomographic model which goes beyond the current ones which only include depth-invariant discontinuities (such as those of the PREM radial density model) and instead includes self-consistently the observed 660 km dynamic topography. As discussed above, our approach will be to assume that tomographic models of the split-mantle parameterization type lead to useful insights on the dynamic role of the 660 km phase discontinuity, irrespective of possible modifications that may be made to them.

Inspection of our results, presented in Figure 6, shows that they are essentially the same for all three tomographic models. Specifically, for no model is there evidence of the local minimum in mass flux that is expected if the phase transition effect is strong (Peltier and Solheim, 1992). This is in spite of the fact, demonstrated in the previous Section, that the split models have characteristics that are in all other respects consistent with this notion. It is however clear on the basis of the wavenumber decomposition of the radial mass flux diagnostic presented in Tackley et al. (1993) that the expected local minimum in the mass flux is defined entirely by the shorter horizontal wavelengths in the variance spectrum. Therefore we cannot expect, and indeed do not find, that the radial mass flux diagnostic determined from a highly truncated tomographic image is a particularly sensitive measure of the extent of layering that may be characteristic of the convective circulation in the modern earth. In what follows, we therefore focus our attention upon another circulation diagnostic which is more sensitive.

3.2 The depth-dependent profile of heat flow by advection

Although previous analyses have been performed of the extent to which the radial heat flow effected by the mantle convective circulation may be recovered from a model based upon seismic tomography (Hager and Clayton, 1989), this diagnostic has only recently been computed for the best presently available tomographic models (Pari and Peltier, 1995). Here, we suggest that this characteristic might provide an especially sensitive way of discriminating between such models. To understand why this diagnostic is expected to be more sensitive to layering than the mass flux we need only inspect its analytical form. Representing by $\mathcal{F}(r)$ the depth-dependent spherical average of the dynamical contribution to the radial heat flow, then

$$\mathcal{F}(r) = \rho\, C_p \int\!\!\int_{\Omega} w\, \delta T\, d\Omega. \tag{11}$$

Here, $\delta T(r,\theta,\phi)$ denotes the perturbation of temperature away from the geotherm (the depth-dependent spherical average of the absolute temperature field T),

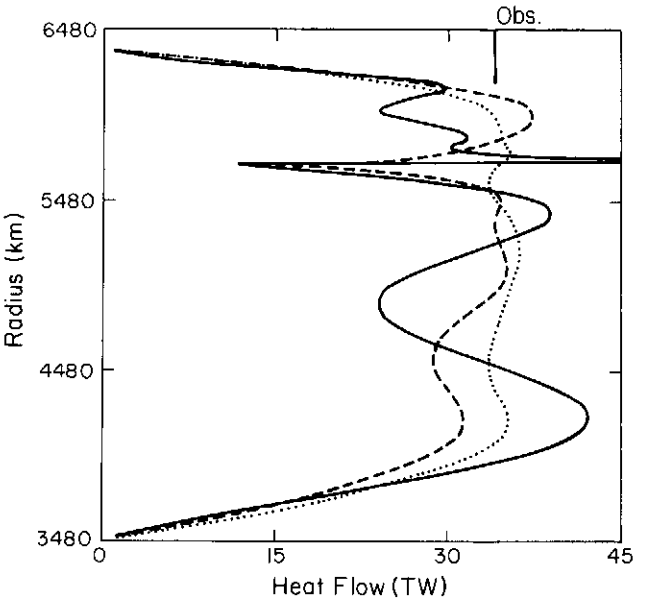

Fig. 7. The advected heat flow $\mathcal{F}(r)$ (text equation 11) as a function of mantle radius. The dotted line corresponds to SH8/WM13, the dashed line to SH8/U4L8 and the solid line to SH12^8/U7L5. We indicate on the upper edge of the figure an average advected heat flow of 34 TW, a value to which 8 TW due to crustal radioactivity must be added to obtain the observed value Pollack et al. (1993).

$\rho(r)$ is the depth-dependent average density taken from PREM (Dziewonski and Anderson, 1981), C_p is the specific heat capacity at constant pressure, and $w(r,\theta,\phi)$ is the radial component of the flow velocity. The temperature fluctuations $\delta T(r,\theta,\phi)$ are derived from a seismic tomography model (say for the relative shear wave anomaly $\delta V_s/V_s$) by employing the relation

$$-\alpha\, \delta T \;=\; \frac{\partial \ln \rho}{\partial \ln V_s} \cdot \frac{\delta V_s}{V_s} \;=\; \frac{\delta \rho}{\rho} \tag{12}$$

in which $\partial \ln \rho / \partial \ln V_s$ is the dimensionless depth dependent seismic conversion factor shown previously in Figure 4, plate b, and $\alpha(r)$ is the depth-dependent coefficient of thermal expansion that is now well constrained for the magnesiowüstite phase by the synchrotron measurements of Chopelas and Boehler (1992). We obtain the radial velocity $w(r,\theta,\phi)$ from the theoretical expression (Pari and Peltier, 1995):

$$w(r,\theta,\phi) \;=\; \sum_{lm} \left[\int_b^a W^l(r,r')\, \delta\rho_{lm}(r')\, dr' \right] \times Y_{lm}(\theta,\phi) \tag{13}$$

in which the density heterogeneity $\delta\rho$ is itself obtained from the tomographic model by using Eq. 12, the integral is carried out over the depth extent of the mantle and the dimensionful functions $W^l(r,r')$ are the viscosity dependent kernels for radial velocity (Pari and

Peltier, 1995) that are determined by employing the anelastically compressible theory of Forte and Peltier (1991). Inspection of the correlation integral $\mathcal{F}(r)$, which will strongly dominate the conductive contribution to the heat flow in regions remote from thermal boundary layers and at high Rayleigh number, demonstrates why it should be a far more sensitive measure of layering than is the radial mass flux. Since the theoretical expression for the latter is (Peltier and Solheim, 1992):

$$\mathcal{M}(r) = \rho \iint_{\Omega} |w| \, d\Omega \,, \tag{14}$$

it is clear that $\mathcal{M}(r)$ is linear in $\delta\rho$ whereas $\mathcal{F}(r)$ is a quadratic function of $\delta\rho$. The fact that $\mathcal{M}(r)$ does not distinguish between models SH8/WM13, SH8/U4L8 or SH12^8/U7L5 follows simply from the very low horizontal resolution of the tomographic models and the linear dependence of the mass flux diagnostic on the internal density perturbation.

That the heat flow diagnostic is a much more sensitive discriminant is demonstrated in Figure 7 in which we compare the $\mathcal{F}(r)$ fields delivered by the three tomography models. On the upper edge of this plate we have marked the observed surface heat flow of 34 TW (Pollack et al., 1993) and we note that away from the expected conductive thermal boundary layers at the core-mantle boundary and the earth's surface in which the radial heat advection tends to zero, models SH8/WM13, SH8/U4L8 and SH12^8/U7L5 all deliver essentially this observed mean heat flow everywhere except at 660 km depth. Model SH8/WM13 shows no drop in advected heat at 660 km depth whereas models SH8/U4L8 and SH12^8/U7L5 show sharp drops in advected heat at this level, just as would be expected if a sharp thermal boundary layer existed at this depth.

We may construe the fact that the depression of the radial heat advection at 660 km depth is essentially identical in models SH8/U4L8 and SH12^8/U7L5 as evidence that this feature might not be entirely an artifact of the parameterization. If it were then we would expect the depth of the depression to be a strong function of the details of the parameterization, which it is not. This feature is also rather independent of other theoretical details (viscosity profile, seismic conversion factor, etc.) that enter in the internal loading theory (Pari and Peltier, 1995). We therefore suggest that the radial heat advection, being a quadratic function of the depth-dependent lateral heterogeneity $\delta\rho$, should be an extremely useful tool with which to "prospect" for the presence of internal boundary layers at depth in the circulation and therefore to reveal more clearly the tendency towards layering.

4 Concluding remarks

4.1 Mantle viscosity and geodynamic self-consistency

Although all three of the above discussed tomographic reconstructions fit the seismic and geodynamic observables equally well, they do differ radically in one important respect and that concerns the dynamical self-consistency of the radial viscosity profile required by the model to fit the geoid (and other dynamical constraints: see references in Forte and Peltier (1987, 1991) and Forte et al. (1993) for a detailed discussion). All models of the geoid so-far produced appear to favour the existence of structure in this profile near 660 km depth. The earliest models by Hager and colleagues (Hager and Clayton, 1989; Hager and Richards, 1989) suggested that this structure consisted of a very large increase in viscosity at 660 km depth by a factor as large as 10^2. The fact that such structure is known not to be compatible with postglacial rebound data (Peltier, 1989; Mitrovica and Peltier, 1993, 1994) if transient rheology may be neglected, led Forte and Peltier (1987, 1991) and Forte et al. (1993) to consider this question anew. Their work has demonstrated, since confirmed by King and Masters (1992) and Pari and Peltier (1995), that radically different viscosity variations across 660 km depth which were also compatible with postglacial rebound constraints were equally capable of satisfying the geoid. This class of models includes that shown in Figure 4, plate a, which is characterized by the presence of a thin soft layer above 660 km depth in which the viscosity is reduced by more than an order of magnitude. This feature appears to be easiest to explain as a consequence of thermal effect (Meade and Jeanloz, 1990; Karato et al., 1990), but see also Sammis and Dein (1974) who suggest that a thin global low-viscosity layer at 660 km depth might have its origin in transformational superplasticity. The low-viscosity notch is explicable in a transparent and straightforward way if a thin thermal boundary layer exists centered upon 660 km depth, in which case it would be expected to be accompanied by an equally thin high viscosity layer immediately below this horizon. That such an internal thermal boundary layer would be expected to induce a local radial viscosity structure such as this was first suggested some years ago (Peltier, 1985). That models with such strong radial viscosity variation only on the small scale of an internal thermal boundary layer do also provide excellent reconciliations of the geoid is extremely important because such models are equally able to reconcile the postglacial rebound constraints, a characteristic that is not shared by models in which the viscosity variation across 660 km depth is on a much larger spatial scale. If only the low-viscosity component of this structure were to exist, we expect that some effect such as transformational superplasticity would have

to be invoked in order to explain it in the context of a whole mantle model of the convective circulation.

4.2 Layered vs whole mantle convection

At this point what we have established, using the different diagnostics of mantle circulation described previously, is that we have two different families of mantle tomography models that satisfy the seismic data similarly but which differ from one-another radically insofar as their implications concerning the importance of the impact on radial mixing of the endothermic phase transformation at 660 km depth. Model SH8/WM13 is generally consistent with the hypothesis that this phase transition has no substantial influence on the flow except when a regional disaggregation of the power spectrum is considered. It is on the basis of such whole mantle tomographic models alone that Jordan et al. (1993) as well as Morgan and Shearer (1993) have argued that mantle circulation is whole mantle in style.

In the present paper, however, we have shown that the current generation of tomographic inversions also allows for a different option. Models SH8/U4L8 and SH12/U7L5 are entirely consistent with the hypothesis that the phase transition is exerting profound influence on the flow. Our interpretation of seismic tomography images in Sections 2 and 3 indicates that this influence is in qualitative accord with a-priori expectations based upon explicit fluid mechanical models that incorporate the phase transition effect (Machetel and Weber, 1991; Peltier and Solheim, 1992; Solheim and Peltier, 1993; Zhao et al., 1992; Tackley et al., 1993; Solheim and Peltier, 1994a, 1994b). The fact that split mantle models provide a self-consistent explanation of the viscosity structure required to simultaneously fit geoid and postglacial rebound constraints might be viewed as a strong geophysical argument in favour of such models.

Even if the thermal boundary layer which is suggested by our application of various diagnostic functions to the split-mantle tomographic models were in part, or even entirely, a consequence of the discontinuous nature of the radial parameterization implemented in these models, it is extremely important to realize that the existence of such a feature is not ruled out by the seismological data but may even be weakly preferred.

It will, however, take the development of a new generation of tomographic models, with better resolution and which perhaps test the stability of the features near 660 km that are imaged in the split mantle parameterizations to convincingly tilt the balance towards one of the two presently viable alternatives. Although we believe model SH12/U7L5 already goes a long way in this direction, a useful test of these ideas would be to construct a tomographic inversion split at an arbitrary depth (at which no a-priori phase transition related structure would be expected to exist on physical grounds) and check whether significant decorrelation is introduced between heterogeneity above and below the split by the choice of parameterization. Such a test has just recently been presented by Li and Romanowicz (1995). They find that the prominent 660 km peak in the variance spectrum that is characteristic of the split-mantle tomographic models does partially survive the displacement of the discontinuity in the radial basis function parameterization. When the split is moved to a depth of 1000 km in their tomographic model SAW12A, a transition zone peak in rms power centered at 660 km depth remains. Further analyses with such models are clearly warranted.

References

Chopelas, A. and R. Bochler, Thermal expansivity in the lower mantle, *Geophys. Res. Lett.,19*, 1982–1986, 1992.

Christensen, U.R., and Yuen, D.A., Layered convection induced by phase transitions, *J. Geophys. Res., 90*, 10291–10300, 1985.

Dziewonski, A. M. and Anderson, D. L., Preliminary reference Earth model, *Phys. Earth Planet. Inter.,25*, 297 356, 1981.

Dziewonski, A. M. and Woodward, R. L., Acoustic imaging at the planetary scale, *Acoustical Imaging, 19*, 785–797, 1992.

Edmonds, A.R., Angular momentum in quantum mechanics, Princeton University Press, Princeton, 1974.

Forte, A. M. and Peltier, W. R., Plate tectonics and aspherical earth structure: the importance of poloidal-toroidal coupling, *J. Geophys. Res., 92*, 3645 3679, 1987.

Forte, A. M. and Peltier, W. R., Viscous flow models of global geophysical observables. I. Forward problems, *J. Geophys. Res.,96*, 20131–20159, 1991.

Forte, A. M., Peltier, W. R., Dziewonski, A. M., and Woodward, R. L., Dynamic surface topography: a new interpretation based upon mantle flow models derived from seismic tomography, *Geophys. Res. Lett.,20*, 225–228, 1993.

Forte, A.M., R.L. Woodward and A.M. Dziewonski, Joint inversions of seismic and geodynamic data for models of three-dimensional mantle heterogeneity, *J. Geophys. Res., 99*, 21857-21877, 1994.

Hager, B. H. and Clayton, R. W., Constraints on the structure of mantle convection using seismic observations, flow models and the geoid, in *Mantle Convection*, W.R. Peltier (ed.), 657–763, Gordan and Breach, New York, 1989.

Hager, B. H. and Richards, M. A., Long-wavelength variations in Earth's geoid: physical models and dynamical implications, *Phil. Trans. R. Soc. Lond., A328*, 309–327, 1989.

Ito, E., Akaogi, M., Topor, L., and Navrotsky, A., Negative pressure-temperature slopes for reaction forming $MgSiO_3$ perovskite from calorimetry, *Science, 249*, 1275–1278, 1990.

Jordan, T. H., Puster, P., Glatzmeier, G. A., and Tackley, P. J., Comparison of seismic earth structures and mantle flow models using radial correlation functions, *Science, 261*, 1427–1431, 1993.

Karato, S., Fujino, K., and Ito, E., Plasticity of $MgSiO_3$ perovskite: the results of microhardness tests on single crystals, *Geophys. Res. Lett.*, *17*, 13–16, 1990.

King, S. and Masters, G., An inversion for radial viscosity structure using seismic tomography, *Geophys. Res. Lett.*,*19*, 1551–1554, 1992.

Li, X.-D. and Romanowicz, B., Global mantle tomography: Evidence for intermittent whole mantle convection, submitted to *Science*, 1995.

Machetel, P. and Weber, P., Intermittent layered convection in a model mantle with endothermic phase change at 670 km, *Nature*, *350*, 55–57, 1991.

Marsh, J. G., Lerch, F. J., Putney, B. H., Felsentreger, T. L., Sanchez, B. V., Klosko, G. B., Patel G. B., Robbins, J. W., Williamson, R. G., Enelis, T. L., Eddy, W. F., Chandler, N. L., Chinn, D. S., Kapoos, S., Rachlin, K. E., Braatz, L. E., and Pavlis, E. C., The GEM-T2 gravitational model, *J. Geophys. Res.*, *95*, 22043–22071, 1990.

Masters, G., Jordan, T. H., Silver, P. G., and Gilbert, F., Aspherical Earth structure from fundamental spheroidal-mode data, *Nature*, *298*, 609–613, 1982.

Masters, T. G., Bolton, H. J., and Shearer, P., Large-scale 3-dimensional structure of the mantle, *EOS*, *73*, 201, 1992.

Meade, C. and Jeanloz, R., The Strength of mantle silicates at high pressure and room temperature: implications for the viscosity of the mantle, *Nature*, *348*, 533–535, 1990.

Mitrovica, J. X. and Peltier, W. R., The inference of mantle viscosity from an inversion of the Fennoscandian relaxation spectrum, *Geophys. J. Int.*, *114*, 45–62, 1993.

Mitrovica, J. X. and Peltier, W. R., Constraints on mantle viscosity based on postglacial uplift data from the Hudson Bay region, *Geophys. J. Int.*, submitted 1994.

Morgan, J. P. and Shearer, P. M., Seismic constraints on mantle flow and topography of the 660-km discontinuity: evidence for whole-mantle convection, *Nature*, *365*, 506–511, 1993.

Olson, P., Silver, P. G., and Carlson, R. W., The large-scale structure of convection in the Earth's mantle, *Nature*, *344*, 209–215, 1990.

Pari, G. and Peltier, W.R., Subcontinental downwellings: the heat flow constraint on tomography based convection models, *EOS*,*74*, 81, 1993.

Pari, G. and Peltier, W. R., The heat flow constraint on mantle tomography based convection models: towards a geodynamically self-consistent inference of mantle viscosity, *J. Geophys. Res.*, in press, 1995.

Peltier, W. R., The LAGEOS constraint on Deep Mantle Viscosity: Results from a new normal mode method for the inversion of viscoelastic relaxation spectra, *J. Geophys. Res.*, *90*, 9411–9421, 1985.

Peltier, W.R., Mantle viscosity, in *Mantle Convection*, W.R. Peltier (ed.), 389–478, Gordan and Breach, New York, 1989.

Peltier, W. R. and Solheim, L. P., Mantle phase transitions and layered chaotic convection, *Geophys. Res. Lett.*,*19*, 321–324, 1992.

Peltier, W. R., Jarvis, G. T., Forte, A. M., and Solheim, L. P., The radial structure of the mantle general circulation, in *Mantle Convection*, ed. W.R. Peltier, 675–815, Gordan and Breach, New York, 1989.

Pollack, H. N., Hurter, S. J., and Johnson, J. R., Heat flow from the Earth's interior: analysis of the global data set, *Rev. Geophys.*,*31*, 267–280, 1993.

Sammis, C.G. and Dein, J.L., On the possibility of transformational superplasticity in the Earth's mantle, *J. Geophys. Res.*, *79*, 2961–2965, 1974.

Shearer, P. M. and Masters, T. G., Global mapping of topography on the 660-km discontinuity, *Nature*, *355*, 791–796, 1992.

Solheim, L. P. and Peltier, W. R., Mantle phase transitions and layered convection, *Can J. Earth Sci.*, *30*, 881–892, 1993.

Solheim, L. P. and Peltier, W. R., Avalanche effects in phase transition modulated thermal convection: A model of Earth's mantle, *J. Geophys. Res.*, *99*, 6997–7018, 1994a.

Solheim, L. P. and Peltier, W. R., Phase boundary deflections at 660-km depth and episodically layered isochemical convection in the mantle, *J. Geophys. Res.*, *99*, 15861-15875, 1994b.

Su, W.-j., Woodward, R. L., Dziewonski, A. M., Degree 12 model of shear velocity heterogeneity in the mantle, J. Geophys. Res., *99*, 6945–6980, 1994.

Tackley, P. J., Stevenson, D. J., Glatzmeier, G. A., and Schubert, G., Effects of an endothermic phase transition at 670 km depth in a spherical model of convection in the Earth's mantle, *Nature*, *361*, 699–704, 1993.

Woodward, R. L., Forte, A. M., Su, W.-j., and Dziewonski, A. M., Constraints on the large scale structure of the Earth's mantle, *Evolution of the Earth and Planets, Geophysical Monograph 74*, IUGG Volume 14, 89–109, 1993.

Woodward, R. L., Dziewonski, A. M., and Peltier, W. R., Comparison of seismic heterogeneity models and convective flow calculations, *Geophys. Res. Lett.*,*21*, 325–328, 1994.

Zhao, W., Yuen, D. A., and Honda, S., Multiple phase transitions and the style of mantle convection, *Phys. Earth Planet. Inter.*, *72*, 185–210, 1992.